MODELLING OF BIPOLAR TRANSISTORS INCLUDING QUASI-SATURATION EFFECTS

A Thesis submitted to the Electrical and Electronic
Engineering Department of BUET, Dhaka,
in partial fulfilment of the
requirements for the degree of
Master of Science in Engineering
(Electrical and Electronic)

SHARIF MOHAMMAD MOMINUZZAMAN

June 1993

"R"
623.814133
1993
MOM

The thesis MODELLING OF BIPOLAR TRANSISTORS INCLUDING QUASI-SATURATION EFFECTS submitted by Sharif Mohammad Mominuzzaman, Roll No. 901333P, Session '88-89 to the Electrical and Electronic Engineering Department of B.U.E.T. has been accepted as satisfactory for partial fulfilment of the requirements for the degree of Master of Science in Engineering (Electrical and Electronic).

BOARD OF EXAMINERS

1. Dr. M. M. Shahidul Hassan
   Associate Professor
   Department of EEE
   B.U.E.T., Dhaka-1000,
   Bangladesh.

   Chairman ____________
   (Supervisor)

2. Dr. Saiful Islam
   Professor and Head
   Department of EEE
   B.U.E.T., Dhaka-1000,
   Bangladesh.

   Member ____________ 13.6.93
   (Ex-officio)

3. Dr. Mohammad Ali Choudhury
   Assistant Professor
   Department of EEE
   B.U.E.T., Dhaka-1000,
   Bangladesh.

   Member ____________ 13.6.93

4. Dr. Shamsuddin Ahmed
   Professor and Head
   Department of EEE
   ICTVTR, Board Bazar,
   Gazipur, Dhaka.

   Member ____________
   (External)

DECLARATION

I hereby declare that this work has been done by me and it has not been submitted elsewhere for the award of any degree or diploma.

Countersigned

(Dr. M. M. Shahidul Hassan)

Supervisor

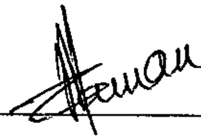

(Sharif Mohammad Mominuzzaman)

ACKNOWLEDGEMENT

The author would like to express his indebtedness and gratitude to his supervisor Dr. M. M. Shahidul Hassan, Associate Professor of Electrical and Electronic Engineering Department, BUET, for his continuous supervision, constant inspiration, endless patience, friendly supervision and invaluable assistance throughout the entire progress of the work.

The author also wishes to express his thanks to Dr. Saiful Islam, Professor and Head, Department of Electrical and Electronic Engineering, BUET, for his support to complete this work successfully.

The author expresess thanks and indebtedness to Dr. Mohammad Ali Choudhury for his incessant assistance, helpful comments and suggestions. Thanks to Mr. Mosaddeque-Ur-Rahman and Mr. Iqbal Yousuf, Lecturer of Electrical and Electronic Engineering Department, BUET, for their encouragement during thesis work.

Finally the author would like to thank all of his friends and colleagues for their constant support and critisism of the research work.

ABSTRACT

Epitaxial $n^+pn^-n^+$ bipolar power transistors offer several advantages over the previously used npn structures. The collector of this type of transistor is more lightly doped than its base. As a result high current effects occur predominantly in the epitaxial collector region. At low voltages, the transistor operates in saturation and when the current is high, a space-charge region is formed in the lightly doped collector region to support the current. Therefore, the need for an understanding the dynamics of the epi-collector under different collector current densities is necessary. In order to investigate the dynamics of the epi-collector transistor, a new approach called 'regional approach' is applied. The whole epi-collector is divided into three regions, namely i) injection region, ii) intermediate region and iii) end region. By applying regional approach, the electric field distributions and the voltage in each of these regions can be determined. Only in the injection region where the electric field is low, the carrier mobility is considered constant. In other cases, nonlinear dependancy is assumed. By using the present model, the different characteristics of bipolar transistors are studied. The model needs simple representation of the physical effects considered and demonstrates its ability to simulate device behaviour. The results obtained by this model are in good agreement with experimental data obtained in an earlier work.

CONTENTS

CHAPTER 1 Introduction

1.1 Epitaxial Bipolar Transistor 1

1.2 Current-voltage relationship under low injection level 3

1.2.1 The Ebers-Moll model 3

1.2.2 The Gummel-Poon model 5

1.3 Current-voltage relationship under high injection level 10

1.4 Summary of the dissertation 13

CHAPTER 2 Current-Voltage Characteristics of Epitaxial Bipolar Transistor

2.1 Introduction 15

2.2 Analysis of epitaxial Bipolar Transistor 16

2.2.1 Lightly doped collector region model 16

2.2.2 Base region model 25

2.3 Conclusion 26

CHAPTER 3 Model Implementation and Results of Epitaxial Bipolar Transistor

3.1 Introduction 27

3.2 Numerical Analysis of Epitaxial Bipolar Transistor 28

3.3 Results 34

3.4 Conclusion 40

CHAPTER 4 Conclusions and Suggestions

4.1 Conclusions 45

4.2 Suggestions 46

References 47

Appendix 49

List of Figures

1.1. A structure of an epitaxial bipolar $n^+pn^-n^+$ power transistor 2

1.2. A circuit diagram of the Ebers-Moll model of bipolar transistor 6

1.3. A circuit diagram of the Gummel-Poon model of bipolar transistor 11

1.4. I_C versus V_{CE} characteristics for a transistor showing ohmic and nonohmic quasi-saturation regions 12

2.1. An one-dimensional $n^+pn^-n^+$ structure of an epitaxial bipolar transistor showing different regions 17

3.1. A flow chart illustrating the procedure for computing current-voltage characteristic 30

3.2. Current voltage characteristic for different base currents of a bipolar transistor 35

3.3. Current-voltage characteristic for different values of $V_{B'E}$ of a bipolar transistor 37

3.4. Collector width as a function of collector-emitter voltage for given values of collector and base current of a bipolar transistor 38

3.5. Base width as a function of collector-emitter voltage for given values of collector and base current of a bipolar transistor 39

3.6. Emitter width as a function of collector-emitter voltage for given values of collector and base current of a bipolar transistor 41

3.7. Emitter area as a function of collector-emitter voltage for given values of collector and base current of a bipolar transistor 42
3.8. Output characteristics comparing compact model simulation and measurements of an npn transistor 43

List of Tables

3.1. Device make-up 44

3.2. Device parameters 44

CHAPTER 1

Introduction

1.1 Epitaxial Bipolar Transistor

Modelling of epitaxial $n^+pn^-n^+$ power transistor is necessary because of its increasing use as high speed switch in power conditioning applications. The epitaxial technique consists of growing a thin, high-purity single-crystal layer of silicon or germanium on a heavily doped substrate of the same material. This augmented crystal forms the collector on which the base and emitter may be diffused through some standard processing [1]. Epitaxial techniques are useful in manufacturing power transistors. For a power transistor switch, the desired features are current-handling capability in the on-state and blocking voltage in the off-state together with switching times and losses. These features can be successfully achieved in an epitaxial transistor. A typical structure of an epitaxial bipolar $n^+pn^-n^+$ power transistor is shown in Fig. 1.1. The region adjacent to the base-collector junction is the most lightly doped and supports the reverse-biased collector-base voltage. Hence, this region essentially determines the breakdown voltage. In regard to the collector thickness W_C, the obvious choice would be to allow the depletion layer to spread freely at the specified open base breakdown voltage BV_{CEO}. But a moderate reduction of W_C less than the unbounded depletion layer width can lead to an advantageous rise in maximum collector current I_C. On the other hand, in order to avoid change of voltage-blocking capability such reduction must be accompanied by a decrease in the collector impurity concentration N_C, thereby increasing the collector resistance.

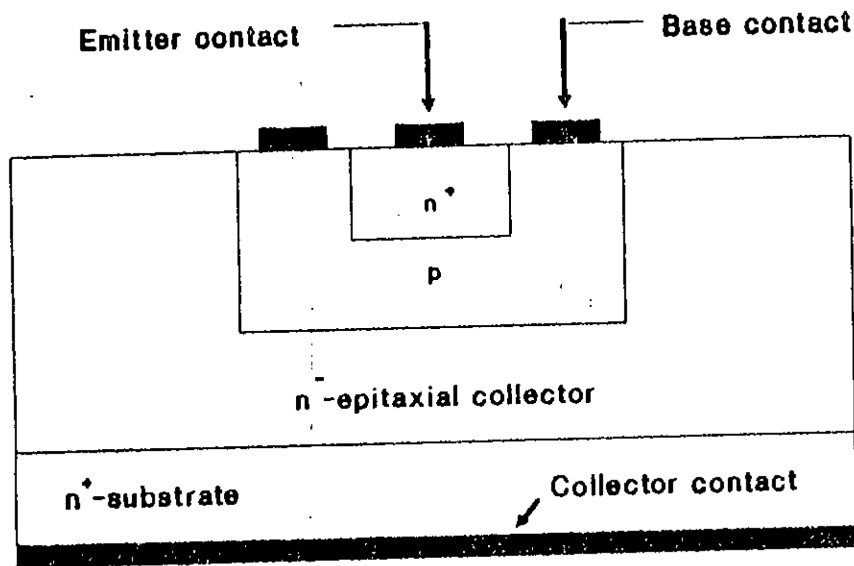

Fig. 1.1. Cross-section of an $n^+pn^-n^+$ epitaxial bipolar transistor

The best performance of transistors demands a combination of high doping levels and thin epitaxial layers to meet the requirement of supporting BV_{CEO} voltage. Optimization of the collector layer in this respect leads to a reach-through condition at breakdown. The heavily doped (n^+) substrate cuts the electric field abruptly at the n^-n^+ interface with zero voltage drop.

Epitaxial techniques offer great versatility for manufacturing power transistors. Multilayered epitaxial transistors may combine some of the advantages of the previous structures.

1.2 Current-voltage relationship under low injection level

Device modelling aims at relating physical device parameters to device terminal characteristics. Device modelling is especially important for integrated circuits, since simple and accurate device models are needed to predict the performances of circuits. Models representing accurate transistors are complex and difficult to study. Therefore, there is a trade-off between accuracy and complexity. Different models are analyzed until recently considering low and high level injection. The most simplified model for low level injection is the Ebers-Moll model [2].

1.2.1 The Ebers-Moll model

Ebers-Moll model is simplified model for bipolar transistor. This model consists of two diodes connected back to back and two current sources. The current sources are driven by the diode currents which are assumed to have ideal characteristics. Forward and reverse-biased diode currents are given by

$$I_F = I_{FO}\left(e^{\frac{qV_{EB}}{kT}} - 1\right) \tag{1.1}$$

$$I_R = I_{RO}\left(e^{\frac{qV_{CB}}{kT}} - 1\right) \tag{1.2}$$

where, I_{FO} and I_{RO} are the saturation currents of the normally forward and reverse-biased diodes, respectively. The terminal currents are,

$$I_E = I_F - \alpha_I I_R \tag{1.3}$$

$$I_C = I_R - \alpha_N I_F \tag{1.4}$$

and

$$I_B = -(1-\alpha_N)\, I_F - (1-\alpha_I)\, I_R \tag{1.5}$$

where, α_N and α_I are the forward and reverse common-base current gains, respectively. Equations (1.1)-(1.5) give relation between terminal currents I_E and I_C and the terminal voltages, V_{EB} and V_{CB}.

Using equations (1.1), (1.2), (1.3) and (1.4), I_E and I_C can be written as,

$$I_E = a_{11}\left(e^{\frac{eV_{CB}}{kT}} - 1\right) + a_{12}\left(e^{\frac{eV_{CB}}{kT}} - 1\right) \tag{1.6}$$

and,

$$I_C = a_{21}\left(e^{\frac{eV_{CB}}{kT}} - 1\right) + a_{22}\left(e^{\frac{eV_{CB}}{kT}} - 1\right) \tag{1.7}$$

Here,

$$a_{11} = I_{FO} \tag{1.8}$$

$$a_{12} = -I_{RO} \tag{1.9}$$

$$a_{21} = -\alpha_N I_{FO} \tag{1.10}$$

$$a_{22} = I_{RO} \tag{1.11}$$

From the reciprocity characteristic of the two-port device,

$$a_{12} = a_{21} \tag{1.12}$$

so that,

$$\alpha_I I_{RO} = \alpha_N I_{FO} \tag{1.13}$$

Fig. 1.2 shows the circuit diagram of the Ebers-Moll model of a bipolar junction transistor.

The Ebers-Moll model was developed based on the following five assumptions (for an npn transistor).

i) Electrons diffuse from emitter to collector,

ii) drift is negligible in the base region,

iii) the emitter current is made up entirely of electrons,

iv) the emitter injection efficiency is unity and

v) the active part of the base and the two junctions are of uniform cross-sectional area.

Current flow in the base is essentially one dimensional from emitter to collector.

In Ebers-Moll model base-narrowing (Early effect) was not incorporated. The model did not consider the collector region in evaluation of current-voltage characteristics of the transistor.

1.2.2 The Gummel-Poon model

The Ebers-Moll model [2] has been the major large-signal model for bipolar transistors since its formulation in 1954. It is based directly on device physics and covers all operating regions, that is, active, saturated and cut-off operation. But various approximations limit the accuracy of the model. In 1957 Beaufoy and Sparkes [3] analyzed the bipolar transistor from a charge control point of view. The charge control model or the equivalent charge control form of the Ebers-Moll model, is directly useful for transient analysis.

As device technology evolved over the years making possible devices of reproducible charateristics and as better understanding was gained in device-theories, many new effects were identified that are not represented by Ebers- Moll model [2]. Among these are a finite, collector-current-dependent output conductance due to basewidth modulation (Early effect) [4], space-charge-layer generation and re-

BASIC MODEL

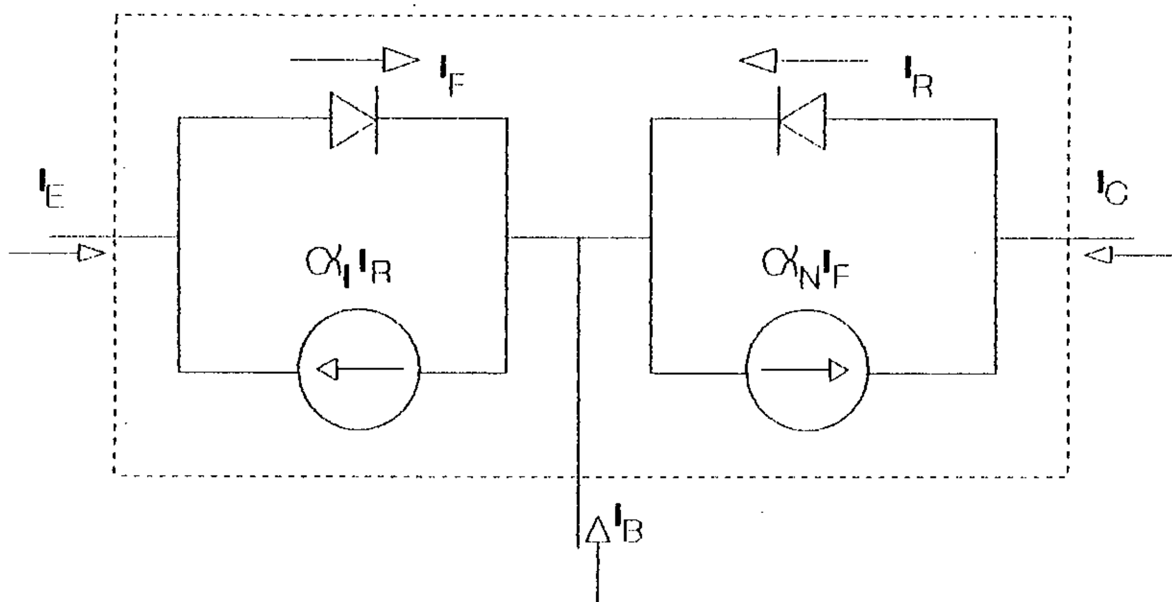

Fig. 1.2. Circuit diagram of the Ebers–Moll model of a bipolar transistor

combination (Sah-Noyce-Shockley effect) [5], conductivity modulation in the base (Webster effect) [6] and in the collector (Kirk effect) [7] and emitter crowding.

The Gummel-Poon model [8] makes use of a general charge-control relation which links junction voltages, collector current and base charge. This charge control relation, used in conjunction with conventional charge control theory, allows many of the effects not contained in the basic Ebers-Moll model to be incorporated in an integral, physical way, in compact form.

To obtain the integral charge relation, consider the current equations,

$$J_n = q\mu_n n \frac{\partial \phi_n}{\partial x} \tag{1.14}$$

and

$$J_p = -q\mu_p p \frac{\partial \phi_p}{\partial x} \tag{1.15}$$

where J_n and J_p are electron and hole current densities, μ_n and μ_p are the elctron and hole mobilities, $\phi_n(\phi_p)$ electron (hole) Fermi level.

The electron and hole concentrations can be given by,

$$n = n_i \exp\left(q(\psi - \phi_n)/kT\right) \tag{1.16}$$

$$p = n_i \exp\left(q(\phi_p - \psi)/kT\right) \tag{1.17}$$

n_i is the intrinsic concentration and ψ is the potential.

The space derivative of the pn product can be written as

$$\frac{d}{dx}(pn) = \frac{q(pn)}{kT}\left(\frac{\partial \phi_p}{\partial x} - \frac{\partial \phi_n}{\partial x}\right) \tag{1.18}$$

Integrating the equation (1.18) from x=0 to x=W, using equations (1.14) to (1.17) and considering negligible recombination, it can be shown [8]

$$pn|_{x=0} - pn|_{x=W} = \frac{J_{CC}}{kT}\int_0^W \frac{n(x)}{\mu_p}dx \tag{1.19}$$

where, J_{CC} is the current density that would flow from emitter to collector if the transistor had unity gain. Substituting equations (1.16) and (1.17) into (1.19) yields

$$exp\left(\frac{q(\phi_p - \phi_n)}{kT}\right)|_{x=0} - exp\left(\frac{q(\phi_p - \phi_n)}{kT}\right)|_{x=W} = \frac{J_{CC}}{n_i^2 kT}\int_0^W \frac{n(x)}{\mu_p}dx \qquad (1.20)$$

In the model the electron imref ϕ_n is considered constant in the base. Therefore,

$$V_{EB} = \phi_p(0) - \phi_n(0) \qquad (1.21)$$

and

$$V_{CB} = \phi_p(W) - \phi_n(W) \qquad (1.22)$$

These voltages differ from terminal voltages by ohmic drops. Equation (1.20) becomes

$$I_{CC} = A_E J_{CC} = qn_i A_2 D_B \left(\frac{e^{\frac{qV_{EB}}{kT}} - e^{\frac{qV_{CB}}{kT}}}{qA_E \int_0^W ndx}\right) \qquad (1.23)$$

where A_E is the active area. The Gummel-Poon model is based on equation (1.20) which links junction voltages, collector current and base charge. The modelling problem reduces to modelling the base charge

$$Q_B = qA\int_0^W ndx \qquad (1.24)$$

which consists of five components :

$$Q_B = Q_{BO} + Q_{JE} + Q_{JC} + Q_{dE} + Q_{dC} \qquad (1.25)$$

where, Q_{BO} is the zero-bias charge, Q_{JE} and Q_{JC} are charges associated with emitter and collector depletion capacitance, Q_{dE} and Q_{dC} are minority-carrier charges associated with emitter and collector diffusion capacitances. As the injection level increases, the diffusion capacitances increase. Thereby giving rise to the high-injection gain degradation. Rewriting equation (1.23), it can be shown

$$I_{CC} = I_F - I_R \qquad (1.26)$$

where,

$$I_F = I_S Q_{BO} \left(\frac{e^{\frac{qV_{EB}}{kT}} - 1}{Q_B} \right) \tag{1.27}$$

$$I_R = I_S Q_{BO} \left(\frac{e^{\frac{qV_{CB}}{kT}} - 1}{Q_B} \right) \tag{1.28}$$

Equations (1.27) and (1.28) resemble equations (1.1) and (1.2) in the Ebers-Moll model. The charge Q_{dE} can be expressed as $B\tau_F I_F$, where τ_F is the lifetime associated with minority carriers in forward current and B is a factor that is usually equal to unity, but may become larger than unity from the Kirk effect. The charge Q_{dC} can be expressed as $\tau_R I_R$, where τ_R is the lifetime of minority carriers in reverse current. The base current is given by

$$I_B = \frac{dQ_B}{dt} + I_{rec} \tag{1.29}$$

where the base recombination current can be separated into two parts,

$$I_{rec} = I_{EB} + I_{CB} \tag{1.30}$$

where,

$$I_{EB} = I_1 \left(e^{\frac{qV_{EB}}{kT}} - 1 \right) + I_2 \left(e^{\frac{qV_{EB}}{m_e kT}} - 1 \right) \tag{1.31}$$

and

$$I_{CB} = I_3 \left(e^{\frac{qV_{EB}}{m_c kT}} - 1 \right) \tag{1.32}$$

In these equations, m_e and m_c are the emitter and collector ideality factors. For ideal currents m_e and m_c are both equal to 1; for depletion-recombination-generation currents, m_e and m_c are both equal to 2. The total emitter and collector currents can be expressed as,

$$I_E = I_{CC} + I_{BB} + \tau_F \left(\frac{dI_F}{dt}\right) + C_{jE} \left(\frac{dV_{EB}}{dt}\right) \quad (1.33)$$

$$I_C = I_{CC} - I_{CB} - \tau_R \left(\frac{dI_R}{dt}\right) + C_{jC} \left(\frac{dV_{EC}}{dt}\right) \quad (1.34)$$

Fig. 1.3 shows the circuit diagram of the Gummel-Poon model, complete with series resistances. Since Q_B is voltage-dependent, the effect of high injection in the base ($\tau_F I_F$ becoming larger than Q_{BO}) is included. The current-induced base push-out (Kirk effect) is represented by the factor B, which is a function of I_C and V_{CB}. The emitter part I_{BE} of the base current is modelled by two diodes in paralled, one ideal and one with an ideality factor $m_e > 1$. This makes the current gain at low current levels bias dependent. The voltage dependence of Q_{jC} ($=c_{jc}V_{CB}$) models the Early effect. Many physical effects have been taken into account through the bias -dependent Q_B.

1.3 Current-voltage relationship under high injection level

Recently, Kull et al. [9] presented a compact model which is an extension of the Gummel-Poon model [8]. This model is applicable to bipolar junction transistors even exhibiting quasi-saturation or base push-out effects. When device with a lightly doped collector region is operated at high injection levels (in the collector region), dc current gain falls sharply from its maximum value. Such an operating regime is generally refered as quasi-saturation. Quasi-saturation can be defined as the region where the internal base-collector metallurgical junction is forward biased, while the external base-collector terminal remains reverse biased. In this mode of operation, minority carriers are injected into the epitaxial region, widening the electrical base of the device and thus reducing current gain and storing excess charge in the epitaxial region. A plot of I_C versus V_{CE} for various fixed base currents is shown in Fig. 1.4 for a typical transistor exhibiting quasi-saturation [9]. This figure shows two distinct quasi-saturation regions, the ohmic and the nonohmic region.

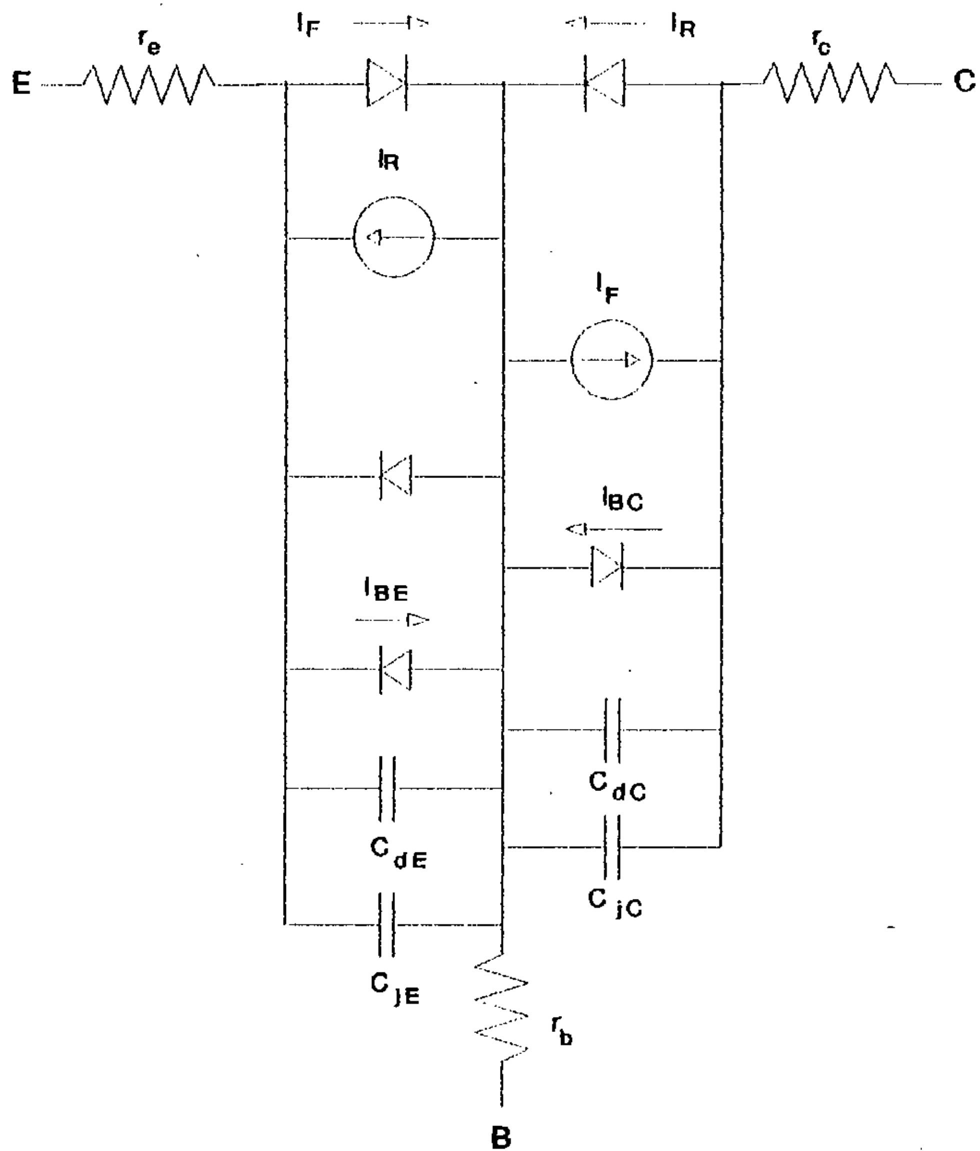

Fig. 1.3. Circuit diagram of the Gummel-Poon model of a bipolar transistor

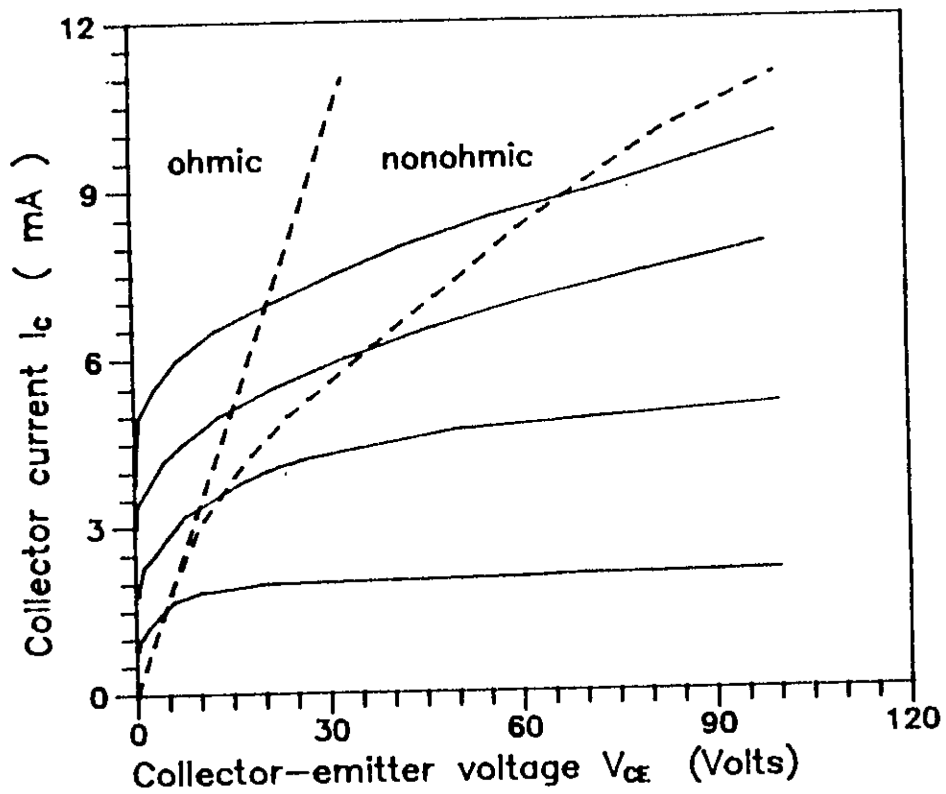

Fig. 1.4. I_C versus V_{CE} characteristics of a transistor. The ohmic and non–ohmic quasi–saturation regions are shown in this graph.

In the ohmic region the locus of points at which the device enters quasi-saturation from the regime of normal forward mode follows a slope approximately equal to the unmodulated epitaxial collector conductance. Above some critical collector current, in the nonohmic region, the device is observed to enter into the quasi- saturation region at voltages higher than the ohmic region locus of points would predict.

The quasi-saturation effect has been investigated by many authors [10, 11, 12, 13] and in general two distinct models have been developed for the ohmic and nonohmic regions of operation. For the ohmic model, the carrier drift velocity is assumed to be linearly proportional to the electric field. For the nonohmic quasi-saturation model, the carriers in the entire collector space-charge region are assumed to be moving at their scattering-limited velocity. In the nonohmic model, Whitter and Tremere [11] have examined the importance of two-dimensional effects, such as current crowding and current spreading. Kumar and Hunter [14] showed that a one-dimensional model is adequate to model the nonohmic quasi-saturation effect. In the present research the model for the epitaxial collector region is derived from physical equations describing semiconductor behavior which are simplified and solved analytically. A single equation results from a steady-state analysis, and it describes the current in the epitaxial region as a function of two junction potentials and three device parameters. These parameters are related to physical quantities such as doping concentrations and carrier mobility. This equation includes the effects of base widening, conductivity modulation and field dependence of carrier velocity. Two additional equations, (defined in terms of one model parameter), represented the excess charge stored in the epitaxial region.

1.4 Summary of the Dissertation

Now a days, epitaxial $n^+pn^-n^+$ structures are extensively used as power transistors [1]. Since in this type of transistors collector is more lightly doped than base, high current effects occur predominantly in the epitaxial collector region. At low voltage, such a transistor operates in saturation and when the current is high, a

space-charge region must form in the lightly doped collector region to support the current. Reported works on epitaxial bipolar transistor did not adequately account these effects. A knowledge of the injected minority carrier density profile in the lightly doped collector region is essential for predicting the transistor currents in the quasi-saturation region. To obtain a accurate profile both diffusion and drift components of the minority carriers are considered.

In chapter 1 of this thesis, the literature survey on bipolar transistors has been undertaken. Recent works on epitaxial power transistors are also reviewed in this chapter.

In chapter 2, a detailed analysis of the work, particularly for collector region, is given. Unlike the previous models, a regional approach rather than charge control approach in evaluating the I-V characteristic of a transistor is employed. The whole collector region is divided into three regions, i.g. i) injection region, ii) intermediate region and iii) end region. The field distribution in each region is determined considering the appropriate boundary conditions. The area under the field distributions within each region will give the voltage. The sum of all these voltages will give the total voltage across the epi-collector. The low electric field is considered in the injection region. The diffusion current in the consecutive two regions were neglected. Since the electric field in region ii) and iii) is high, this is a good approximation. In this chapter, an analysis is also given for the condition $V_{CE} < V_{BE}$ i.e. the transistor is saturated. Recent model based on the Gummel-Poon model presented by Hanggeun and Fossum [15] has failed to incorporate this mode of operation in their model. The present model incorporates the recent study on the base of the transistor.

In chapter 3, a computer program using iterative scheme is developed to study the characteristic of the transistor. Numerically obtained characteristics are found to be fruitful with experimental results.

CHAPTER 2

Current Voltage Characteristics of Epitaxial Bipolar Transistor

2.1 Introduction

In modern bipolar transistors, the collector is more lightly doped than the base. The high-current effects occur predominantly in the epitaxial collector region. These effects are empirically, and inadequately accounted for in the existing bipolar transistor models. Recently, Kull et al. [9] proposed a dc model which retains the ideas of Gummel-Poon model [8] and includes quasi-saturation device physics. Kull's compact extension, however, is not applicable in general because of the assumption that the entire epitaxial collector region is quasi-neutral. The model is only useful for high voltage (thick-epi) transistors and produce but yields erroneous predictions when applied to VLSI transistors. Hanggeun and Fossum [15] extended Kull's model to account for the possible existence of the current-induced space-charge region in the epitaxial collector. Their model did not include the saturation condition, i.e. $V_{CE} < V_{BE}$ and like other existing models requires parameters extracted from measurements. On the other hand, the proposed model in this work requires only physical parameters such as device make-up.

The present model employs a regional approach rather than previously used charge-control approach. In a bipolar transistor at high currents and low base-collector voltages, an injection region in the collector adjacent to mettalurgical collector-base junction is found to form. In the remaining part of the collector the minority carriers behave as ohmic, tepid or even as hot carriers moving with the

scattering limited drift velocity. A detailed description of all possible carrier and field distributions within the collector and their dependence on current and voltage, as well as, on doping level and width of the collector are given. The base minority carrier density at the junction edge is related with the base-collector junction voltage for all injection levels.

The proposed model includes device physics such as base push-out, collector conductivity modulation and voltage drops in low and high field collector regions under all injection levels. Comparisons of model predictions with measurements available in the literature are included.

2.2 Analysis of Epitaxial Bipolar Transistor

2.2.1 Lightly Doped Collector Region Model

A one-dimensional $n^+pn^-n^+$ structure of an epitaxial bipolar transistor is shown in Fig. 2.1. At relatively low collector voltages and high collector currents, injection model must be used. Both the base drive and the collector-emitter voltage V_{CE} will determine whether the transistor operates in quasi-saturation or active mode of operation. For operation in quasi-saturation, the collector can be divided into three different regions. The regions are, i) an injection region, ii) an intermediate region and iii) an end region. Different regions of the collector will be treated subsequently.

i) Injection Region ($x \leq x_1$)

The electric field in this region is low and the carrier mobility is independent of the electric field. Both types of carriers are important, because there exists a space-charge neutrality. That is:

$$p + N_C \approx n \tag{2.1}$$

and

$$\frac{dp}{dx} = \frac{dn}{dx} \tag{2.2}$$

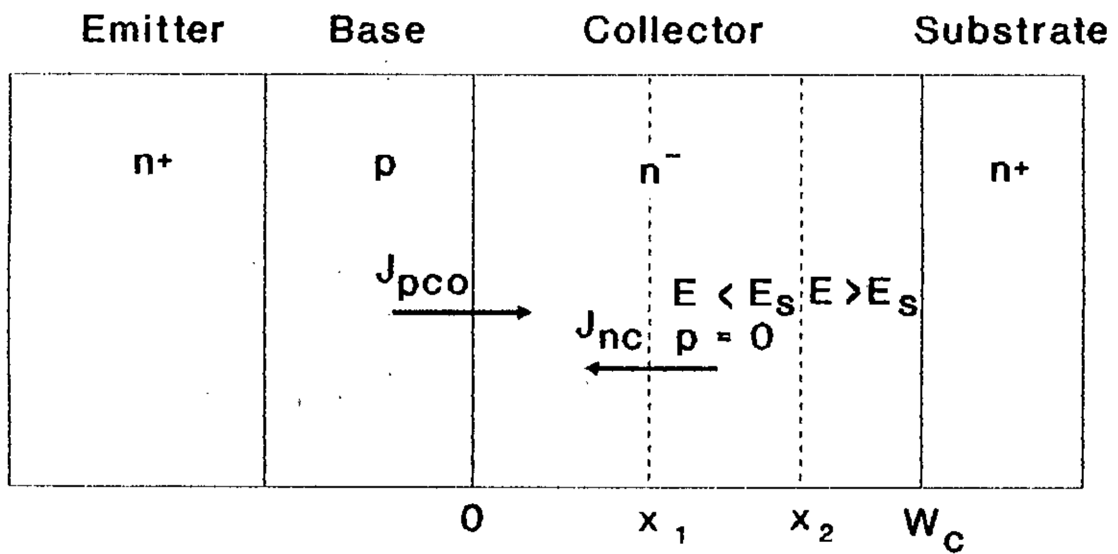

Fig. 2.1. A one-dimensional $n^+pn^-n^+$ structure of an epitaxial bipolar transistor

For high current gain, minority carrier current in the epitaxial collector can be neglected. For npn transistor, the above assumtion gives,

$$J_{pc} = 0 \tag{2.3}$$

To satisfy the condition $J_{pc} = 0$, the drift component must be equal to the diffusion component having flow in the opposite directions. Total current due to minority carrier is the sum of drift and diffusion currents. Therefore,

$$J_{pc} = q\mu_p p E(x) - qD_p \frac{dp}{dx} \tag{2.4}$$

Substituting $J_{pc} = 0$ in equation (2.4), it can be shown that,

$$E(x) = V_T \frac{1}{p(x)} \frac{dp}{dx} \tag{2.5}$$

The other basic equations, for one-dimensional geometry, are

$$-J_{nc} = q\mu_n n E(x) + qD_n \frac{dn}{dx} \tag{2.6}$$

$$\frac{dE}{dx} = \frac{q}{\epsilon}(p + N_C - n) \tag{2.7}$$

Substituting the expression of E(x) of equation (2.5) in equation (2.6) using the relationship,

$$p = n - N_C$$

it can be shown that,

$$-J_{nc} = qD_n \frac{2n - N_C}{n - N_C} \frac{dn}{dx} \tag{2.8}$$

Rearranging equation (2.8) one can obtain,

$$-\frac{J_{nc}}{qD_n} dx = \frac{2n - N_C}{n - N_C} dn \tag{2.9}$$

Integrating equation (2.9) with $I_C = -J_{nc}A_e$, (I_C is the collector current, N_C is the collector doping density and A_e is the emitter area) it can be shown that,

$$x = \frac{2qD_n A_e}{I_C}\left(n_o - n + \frac{1}{2}N_C \ln\left(\frac{n_o - N_C}{n - N_C}\right)\right) \tag{2.10}$$

where, n_o is the electron concentration at the collector side of the collector-base junction.

The expression for electric field E(x) derived from equations (2.1), (2.2), (2.5) and (2.8), can be expressed as,

$$E(x) = -\frac{I_C}{q\mu_n A_e}\left(\frac{1}{2n - N_C}\right) \tag{2.11}$$

and voltage across the injection region derived from equations (2.1), (2.2) and (2.5) is,

$$\begin{aligned} V_{inj} &= -\int_0^{x_1} E(x)dx \\ &= -\int_{n_0}^{n_1} V_T \frac{1}{n - N_C} dn \\ &= V_T \ln\left(\frac{n_o - N_C}{n_1 - N_C}\right) \end{aligned} \tag{2.12}$$

where, n_1 is the electron density at the end of the injection region i.e. at $x = x_1$.

Once x_1, n_o and n_1 are known, eqns.(2.1)-(2.12) completely describe the situation in the injection region. The concentration n_1 can be calculated in connection with the intermediate region. For determination of n_o, the value of $V_{CB'}$ (internal collector-base voltage) is required.

At high injection prevailing both in the base and the collector, hole (electron) concentration at the collector side of the collector-base junction p_o (n_o) can be shown to be of the following form by applying the law of junction (Appendix A),

$$p_o = \frac{AN_B\left(1 + A\frac{N_C}{N_B}e^{-\frac{V_{CB'}}{V_T}}\right)e^{-\frac{V_{CB'}}{V_T}}}{1 - A^2 e^{-\frac{2V_{CB'}}{V_T}}} \tag{2.13}$$

and

$$n_o = N_C + p_o \tag{2.14}$$

where, $A = \frac{n_i^2}{N_B N_C}$, N_C (N_B) is the carrier concentration in the collector (base) region and n_i is the intrinsic carrier concentration for silicon. At low injection condition in the base, equation (2.13) reduces to,

$$p_o = \frac{n_i^2}{N_C} \exp\left(-V_{CB'}/V_T\right) \tag{2.15}$$

where, $V_{CB'}$ is positive if the junction is reverse-biased.

When the transistor is saturated, i.e. $V_{CE} < V_{BE}$, the whole collector is conductivity modulated and the width of the injection region x_1 will become equal to the collector width W_C. The electron concentration can then be determined if $V_{CB'}$ is known. In other situations, the first region is terminated at the plane $x = x_1$, where the neutrality condition (2.1) is no longer self-consistent, in particular we have chosen the following condition to define the value of x_1

$$\frac{\epsilon}{q}\frac{dE}{dx}\Big|_{x=x_1} = N_C - n(x_1) \tag{2.16}$$

The holes are neglected ($p(x_1) = 0$). There is a discontinuity in $p(x)$ at $x = x_1$, but $n(x)$ is continuous at this point. Substitution of (2.8) and (2.11) in (2.16) results in an equation for n_1 and can be written as,

$$n_1 = \frac{1}{2}N_C + \frac{1}{2qD_n A_e}\left(2D_n V_T A_e \epsilon I_C{}^2\right)^{\frac{1}{2}} \tag{2.17}$$

If the values of N_C, D_n, A_e and I_C are known then n_1 can be calculated from equation (2.17). Inserting n_1 in eqn. (2.10) leads to an equation for x whose solution is the boundary of the first region x_1.

ii) Intermediate Region ($x_1 \leq x \leq x_1 + x_2$)

This is a transition region from the cold electron regime of the injection region to the hot electron regime of the following regions. In this region, the electron diffusion current is neglected. The excess holes are also neglected in Poisson's equation. The electron density decreases from n_1 to n_2. Space-charge neutrality does not exist in this region. The boundary condition comes from the requirement of continuity of the electric field across the plane $x = x_1$, $E(x_1^+) = E(x_1^-) = E_1$.

In this region, the electron velocity is assumed to be related to the field [16] by the relationship,

$$\frac{1}{v_n} = \frac{-1}{\mu_n E} + \frac{1}{v_{sn}} \qquad where, \qquad E < E_s \tag{2.18}$$

where, E_s is the field for which the velocity takes the scatterring limited value v_s and v_{sn} is an adjustable parameter which is chosen to obtain $v_n(E_s) = v_s$. For electron, the scattering limited velocity is assumed to be equal to 10^7 cm/sec and the electric field E_s is considered to be 2.5×10^4 V/cm [16].

From Poisson's equation we can calculate voltage across intermediate region. That is,

$$\frac{dE}{dx} \approx \frac{q}{\epsilon}(N_C - n) \tag{2.19}$$

By defining,

$$J_1 = qv_s N_C$$

$$J_n = qv_n n$$

$$a = \frac{J_C}{\mu_n \epsilon_s}$$

$$b = \frac{1}{\epsilon v_s}\left(\frac{J_1}{v_s} - \frac{J_C}{v_{sn}}\right)$$

and

$$\frac{a}{b} = \frac{J_C}{q\mu_n\left(\frac{J_C}{qv_m} - N_C\right)}$$

equation (2.19) becomes,

$$\frac{dE}{dx} = \frac{a}{E} - b \tag{2.20}$$

The solution of Poisson's equation is,

$$E_1 - E + \frac{b}{a}\ln\left(\frac{\frac{a}{b} - E}{\frac{a}{b} - E_1}\right) = b(x - x_1) \tag{2.21}$$

The boundary value n_2 depends on the situation in the end region. That is,

$$n_2 = N_C \qquad for \qquad J_C \leq J_1 \tag{2.22}$$

and

$$n_2 = \frac{J_C}{J_1}N_C \qquad for \qquad J_C > J_1 \tag{2.23}$$

For $J_C \leq J_1$, the voltage of the intermediate region is given by,

$$\begin{aligned} V_2 &= -\int_{x_1}^{x_2} E dx \\ &= -\int_{E_1}^{E_2} \frac{E}{\frac{dE}{dx}} dE \end{aligned} \tag{2.24}$$

Substituting $\frac{dE}{dx}$ from equation (2.20) and after simplifying,

$$V_2 = \frac{1}{b}\left(\frac{1}{2}(E_2^2 - E_1^2) + \frac{a}{b}(E_2 - E_1) + \frac{a^2}{b^2}\ln\frac{E_2 - \frac{a}{b}}{E_1 - \frac{a}{b}}\right) \tag{2.25}$$

For the condition of collector current specified, the width of the intermediate region is found by integrating equation (2.20) within the boundary x_1 and x_2. After simplification we get,

$$x_2 = \frac{1}{b}\left((E_2 - E_1 + \frac{a}{b}\ln\frac{\frac{a}{b} - E_2}{\frac{a}{b} - E_1}\right) \tag{2.26}$$

where, E_2 is the electric field at the end of the intermediate region i.e. at $x = x_1+x_2$. The value of E_2 depends on the situation in the end region.

On the other hand, in the case of $J_C > J_1$, with similer calculation as before, the voltage and the width of the intermediate region is found to be,

$$V_2 = \frac{-1}{b}\left(\frac{1}{2}(E_s^2 - E_1^2) + \frac{a}{b}(E_s - E_1) + \frac{a^2}{b^2}\ln\frac{E_s - \frac{a}{b}}{E_1 - \frac{a}{b}}\right) \tag{2.27}$$

and

$$x_2 = \frac{-1}{b}\left((E_1 - E_s - \frac{a}{b}\ln\frac{E_s - \frac{a}{b}}{E_1 - \frac{a}{b}}\right) \tag{2.28}$$

Therefore, the voltage and the width of the intermediate regin can be calculated if J_C, J_1, E_1, E_s or E_s, v_s and v_{sm} are known from equation (2.25) and (2.26) for J_C $< J_1$ and from equation (2.27) and (2.28) for $J_C > J_1$.

iii) End Region ($x_1 + x_2 \leq x \leq W_C$)

In this region,

i) When $J_C \leq J_1$, field and carrier density are constant. Therefore, $n_2 = N_C$ and $E(x) = E_2$. Substituting $E(x) = E_2$ in equation (2.18), the expression for electric field takes the form,

$$E_2 = -\frac{1}{\mu_n\left(\frac{1}{v_n} - \frac{1}{v_m}\right)} \tag{2.29}$$

With $J_1 = qv_sN_C$ and $J_C = qv_{sn}n$ equation (2.29) becomes,

$$E(x) = E_2 = -k\rho J_C \tag{2.30}$$

where, $k = \frac{1}{1 - \frac{J_C v_s}{J_1 v_{sm}}}$

ii) When $J_C > J_1$, the carrier density and field are no longer constant. Carrier density is given by $n_2 = \frac{J_C}{J_1} N_C$, and electric field $E(x)$ increases with a constant slope of $\frac{qN_C}{\epsilon}\left(\frac{J_C}{J_1} - 1\right)$

For $J_C < J_1$, the voltage and width can be written as,

$$V_3 = E_2 x_3 \tag{2.31}$$

Replacing E_2 by equation (2.30) and simplifying equation (2.31) it can be found that,

$$V_3 = \frac{v_s x_3}{\mu_n \left(\frac{J_1}{J_C} - \frac{v_s}{v_{sn}}\right)} \tag{2.32}$$

The width of the end region is given by,

$$x_3 = W_C - x_1 - x_2 \tag{2.33}$$

For $J_c > J_1$,

$$V_3 = E_s x_3 + \frac{qN_C}{2\epsilon}\left(\frac{J_c}{J_1} - 1\right) x_3^2 \tag{2.34}$$

The voltage and width of the end region can be obtained from equation (2.32) for $J_C < J_1$ and from equation (2.34) for $J_C > J_1$ if v_s, v_{sn}, J_1, J_C and x_3 are known.

The limit of quasi-saturation mode is reached when $x_1 = 0$. This results for different current densities in :

$$V_{CB} = I_B R_B + k\rho W_C J_C \qquad for \qquad J_C \leq J_1 \tag{2.35}$$

and

$$V_{CB} = I_B R_B + E_s W_C + \frac{qN_C}{2\epsilon}\left(\frac{J_C}{J_1} - 1\right) W_C^2 \qquad for \qquad J_C \geq J_1 \tag{2.36}$$

where, I_B is the base current, R_B is the extrinsic base resistance and V_{CB} is the external voltage between collector and the base terminals.

2.2.2 Base Region Model

In d.c. analysis models, the collector region model as proposed in the previous section need to be incorporated with the existing base model. The base current density J_B can be modelled as the current density J_{pe} injected on the base into the emitter. If the recombination within the base is neglected J_B can be given by [17],

$$J_B = J_{pe} = \frac{qD_p}{G_E} n_{ie}^2 \left(e^{\frac{V_{BE}}{V_T}} - 1 \right) \tag{2.37}$$

where,

$$G_E = \int_0^{W_E} N_E(x) dx \tag{2.38}$$

$N_E(x)$ is the emitter doping concentration and n_{ie} is the effective intrinsic concentration including band gap narrowing effect [18].

$$n_{ie} = 1.4 \times 10^{10} exp \left(.433 \sqrt{\frac{N_E}{10^{18}}} \right) \tag{2.39}$$

Recently, Hurkx [19] has studied the velocity saturation effects on the minority carrier transport in the base of a bipolar transistor. An improved expression of the electron current density J_n is derived

$$J_n = \frac{q n_{io}^2 \left(e^{\frac{V_{BE}}{V_T}} - e^{\frac{V_{CB}}{V_T}} \right)}{G_b} \tag{2.40}$$

where, the Gummel number with velocity saturation is given by [19],

$$G_b = G_\infty + \frac{m}{r v_s} \left(\frac{p}{\left(\frac{n_{ie}}{n_{io}} \right)^2} \right) \tag{2.41}$$

where, G_∞ is the base Gummel number without velocity saturation. For a inhomogeneously doped base it is found that $r \approx 0.75$ [19]. The dopant-dependence of n_{ie}/n_{io} is given in [20].

For epitaxial $n^+pn^-n^+$ bipolar transistor, the base is not uniformly doped.

Graaff et. al. [21] have derived analytical formulla for the collector current considering the doping profile approximated by,

$$N_B(x) = N_0 e^{-\frac{tx}{W_B}} \tag{2.42}$$

where, t is a measure of the strength of the built-in field. The neutral base lies between 0 and W_B. They have established equations for collector current I_C both for low and high injection conditions. The detailed analysis are given in [21].

Using the equations derived in this chapter, the $I_C - V_{CE}$ characteristics of an epitaxial $n^+pn^-n^+$ bipolar transistor as a function of I_B (or V_{CB}) can be obtained. In next chapter, a procedure for obtaining the characteristics are given.

2.3 Conclusion

The current-voltage characteristics of a bipolar transistor have been modelled based on the relevant device physics associated with the free carrier transport within the collector layer. The proposed model covers the saturation, quasi-saturation and active mode operations. The results obtained by the model simulation are in good agreement with the experimental data reported in a literature.

CHAPTER 3

Model Implementation and Results of Epitaxial Bipolar Transistor

3.1 Introduction

The epitaxial $n^+pn^-n^+$ transistor is extensively used as power transistors. Since this type of transistor, the collector is more lightly doped than the base, the high current effects occur predominantly in the epitaxial collector region. At low voltages, the transistor operates in saturation and when the current is high, a space-charge region is formed in the lightly doped collector region to support the current. To study this phenomena a regional approach is applied in evaluating the I-V characteristics of the transistor. The whole collector region is divided into three regions, i.e. i) injection region, ii) intermediate region and iii) end region. The field distributions in each region is determined considering the appropriate boundary conditions. The area under the field distributions within each region will give the voltage across that region. The sum of all these voltages will give the total voltage across the epi-collector. The low electric field is considered in the injection region. The diffusion current in the consecutive two regions were neglected.

A computer program using iterative scheme is developed to study the characteristics of transistors. The equations which are used during numerical analysis together with their derivations have been presented in chapter two. We have developed an algorithm of the computer program for model simulation which is elaborated sequentially.

3.2 Numerical Analysis of Epitaxial Bipolar Transistor

Injection model is used at relatively low collector voltage. For operation in quasi-saturation, the collector is divided into i) injection region, ii) intermediate region and iii) an end region. The relevant equations are derived in chapter two for numerical evaluation of I_C versus V_{CE} characteristic. The flow chart of the computation is shown in Fig. 3.1. Total algorithm is divided into twenty two steps. The steps are as shown below:

1. Start the program.

2. Read some necessary coefficients. These coefficients include electron charge (q), base width (W_B), collector width (W_C), emitterwidth (W_E), emitter area (A_e), doping concentrations in emitter, collector and base, scattering limited velocity etc.

3. Specified base current (I_B), collector current (I_C) and ERROR (tolerance).

4. Guess internal collector-base voltage $V_{CB'}$.

5. Calculate collector junction built-in potential (V_{BILT}).

6. Compare V_{BILT} with $V_{CB'}$. If $|\ (V_{CB'})\ | \geq |(V_{BILT})|$ than choose new $V_{CB'}$.

7. Calculate hole concentration (p_o) and electron concentration (n_o) at the base-collector junction at collector side, collector current density (J_C), width of the injection region (x_1) and majority carrier concentration at the boundary of the injection region (n_1).

8. Justify for x_1. If x_1 greater than or equal to the collector width W_C then recalculate n_1.

9. Calculate electric field at the boundary of the injection region (E_1), voltage across the injection region (V_1), electron concentration in emitter at the base

side of the emitter-base junction (n_E) and internal voltage across base-emitter terminals ($V_{B'E}$).

10. Justify for $V_{B'E}$. If $V_{B'E}$ greater than V_{BILT}, choose new I_C and repeat from step (3).

11. Calculate effective intrinsic concentration in emitter (n_{ie}), maximum collector current (I_{CMAX}), and base current (I_B).

12. Compare the calculated value of I_B to specified value of I_B.

13. Calculate ERROR. ERROR $= |\frac{I_B(calculated) - I_B(specified)}{I_B(specified)}|$.

14. If ERROR greater than a constant given in step (2) than modify the value of internal collector-base potential $V_{CB'}$ and repeat from step (6).

15. Check the width of the injection region (x_1) with the collector width (W_C). If x_1 greater than W_C than calculate V_{CE} and print 'Hard saturation'. Stop the program.

16. Print 'Quasnt 'Quasi-saturation'.

17. Calculate collector current density (J_1) at scattering limited velocity.

18. If collector current density (J_C) less than or equal to J_1 then calculate electric field in the intermediate region (E_2) and width of the intermediate region (x_2). a) If (x_1+x_2) greater than or equal to W_C than calculate E_2, V_2, V_{CE}, V_{CB}. Print 'Quasi-saturation-1'. Stop the program. b) Calculate V_2, V_3, V_{CE}, V_{CB}. Print 'Quasi-saturation-2'. Stop the program.

19. Calculate E_3, x_2.

20. If $x_1 + x_2$ greater than or equal to W_C than calculate V_2, V_{CE}, V_{CB}. Print 'Quasi-saturation-3'. Stop the program.

21. Calculate V_2, V_3, V_{CE}, V_{CB}. Print 'Quasi-saturation-4'.

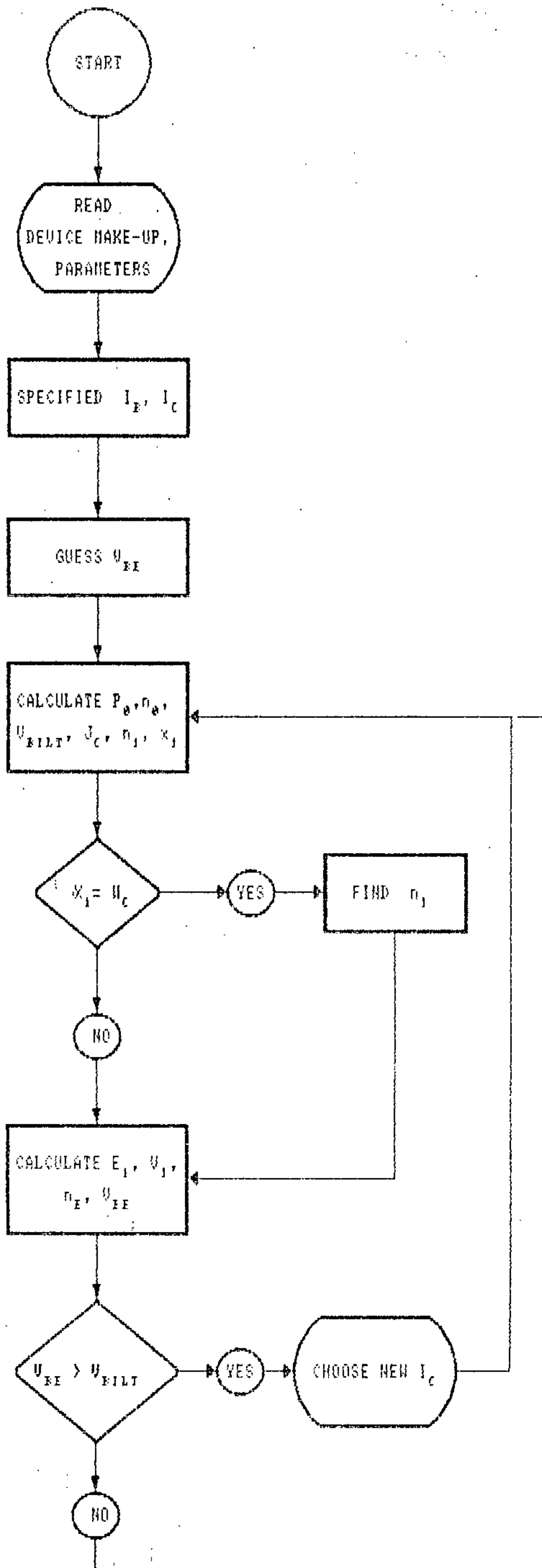
START
READ
DEVICE MAKE-UP,
PARAMETERS
SPECIFIED I_E, I_C
GUESS V_{BE}
CALCULATE P_0, n_0,
V_{BILT}, J_C, n_1, x_1
$X_1 = W_C$
YES
FIND n_1
NO
CALCULATE E_1, V_1,
n_E, V_{BE}
$V_{BE} > V_{BILT}$
YES
CHOOSE NEW I_C
NO

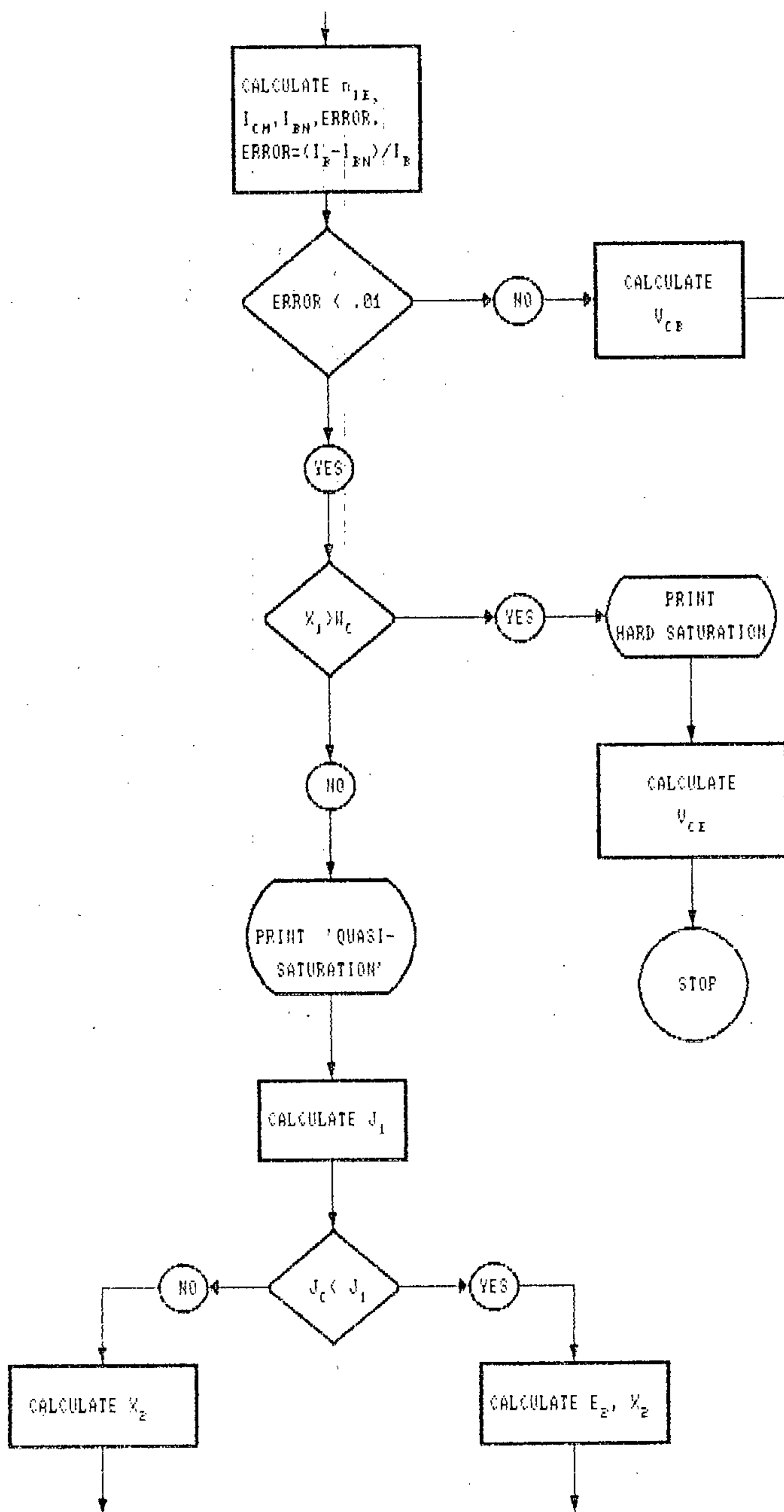
CALCULATE n_{1E}, I_{CN}, I_{BN}, ERROR, ERROR=$(I_B - I_{BN})/I_B$
ERROR < .01
NO
CALCULATE V_{CB}
YES
$X_1 > W_C$
YES
PRINT HARD SATURATION
CALCULATE V_{CE}
STOP
NO
PRINT 'QUASI-SATURATION'
CALCULATE J_1
$J_C < J_1$
NO
YES
CALCULATE X_2
CALCULATE E_2, X_2

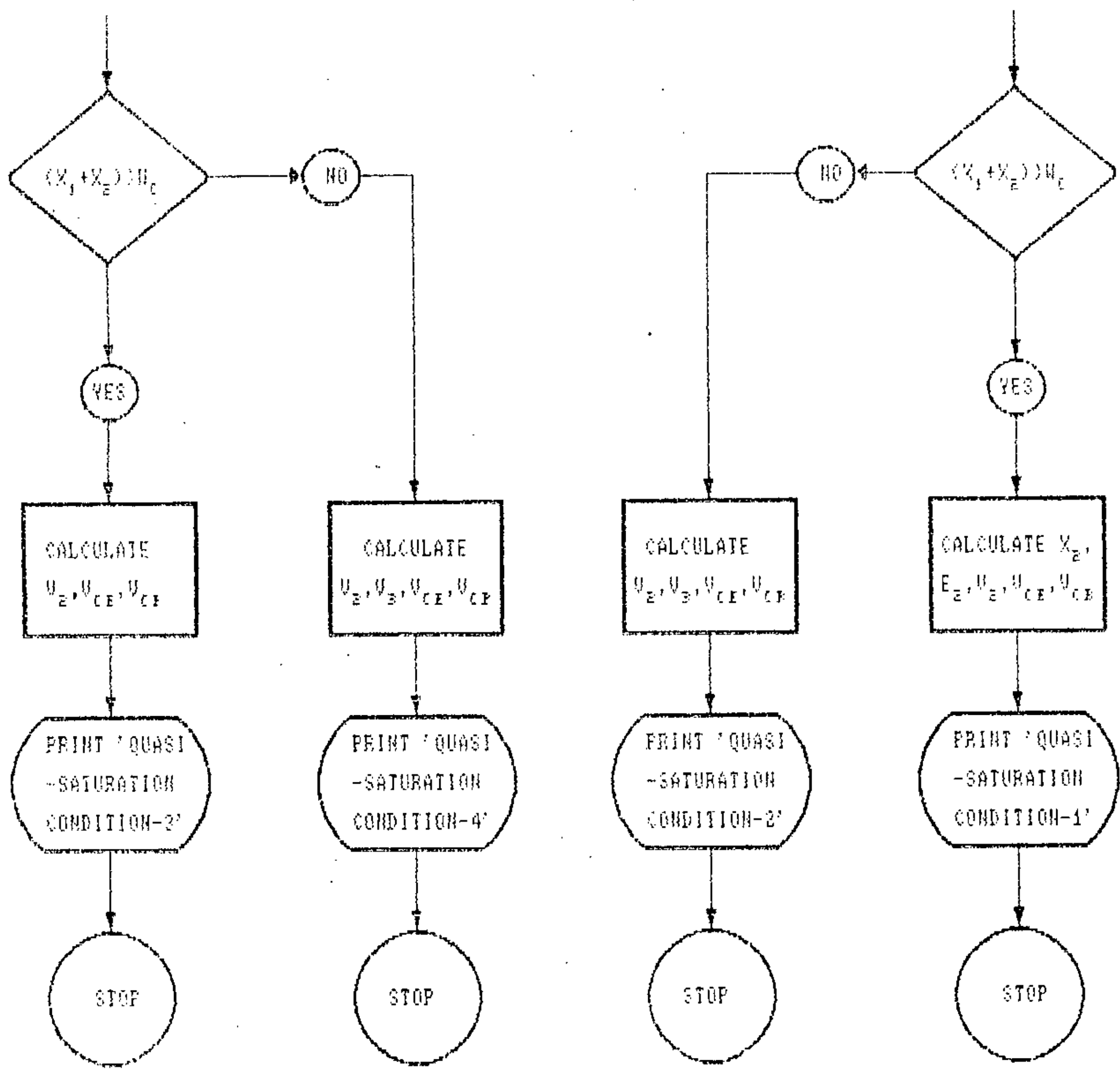

Fig. 3.1. A flow chart illustrating the procedure for computing current-voltage characteristics.

22. Stop the program.

At high injection prevailing both in the base and the collector, p_o is calculated from the equation (2.13). For convenience, the equation is rewritten here.

$$p_o = \frac{AN_B\left(1 + A\frac{N_C}{N_B}e^{-V_{CB'}/V_T}\right)e^{-V_{CB'}/V_T}}{1 - A^2e^{-2V_{CB'}/V_T}} \tag{3.1}$$

and n_o is calculated from the equation,

$$n_o = p_o + N_C \tag{3.2}$$

The width of the injection region x_1 is calculated from the equation (2.10) by substituting the value of n is equal to n_1 . The value of n_1 is obtained from equation (2.17). The electron concentration n_E in emitter is calculated by applying Regula-Falsi method. With the calculated parameter values and using different equations of chapter two we can calculate the value of E_1, V_1, $V_{B'E}$, V_{BILT}, n_{ie}, I_{CM}, I_{BN}. By comparing calculated internal base-collector voltage to the guess internal base-collector voltage, new base-collector voltage and other parameters corresponding to this new value is recalculated. Then injection region is compared with the collector width. If x_1 is greater than W_C then the device drives in saturation and V_{CE} is calculated from,

$$V_{CE} = V_{CB'} + V_{B'E} + V_1 \tag{3.3}$$

Otherwise, the device is in quasi-saturation. By defining,

$$J_1 = qv_sN_C \tag{3.4}$$

J_1 is compared with collector current density J_C. If collector current density is greater than J_1 and $x_1 + x_2$ is greater than or equal to W_C then,

$$V_{CE} = V_{CB'} + V_{B'E} + V_1 + V_2 \tag{3.5}$$

If collector current density is greater than J_1 and $x_1+x_2 < W_C$ then V_{CE} is calculated from,

$$V_{CE} = V_{CB'} + V_{B'E} + V_1 + V_2 + V_3 \tag{3.6}$$

But V_{CE} is calculated in different way if J_C less than or equal to J_1. In this case $x_1 + x_2$ is compared to W_C. If W_C is greater, then

$$V_{CE} = V_{CB'} + V_{B'E} + V_1 + V_2 + V_3 \tag{3.7}$$

Otherwise,

$$V_{CE} = V_{B'E} + V_{CB'} + V_1 + V_2 \tag{3.8}$$

In the above, V_1, V_2, V_3 are calculated from different equations for different values of V_{CE}.

3.3 Results

With the numerically calculated parameters from computer program, different characteristics are obtained.

Fig. 3.2 shows collector current as a function of collector-emitter voltage with different base currents. For higher base current, the collector current is higher for same collector-emitter voltage V_{CE}. This situation can be explained with the following equations [17]:

$$I_C = \frac{qD_{nb}A_e}{W_B}\left(2\left(n_E - n_p\right) - N_B ln\frac{n_E + N_B}{n_p + N_B}\right) \tag{3.9}$$

$$n_p = .5N_B + .5N_B\sqrt{1 + \frac{p_0\left(p_0 + N_C\right)}{N_B^2}} \tag{3.10}$$

$$J_B = \frac{qD_p}{G_E}n_{ie}^2\left(e^{\frac{V_{BE}}{V_T}} - 1\right) \tag{3.11}$$

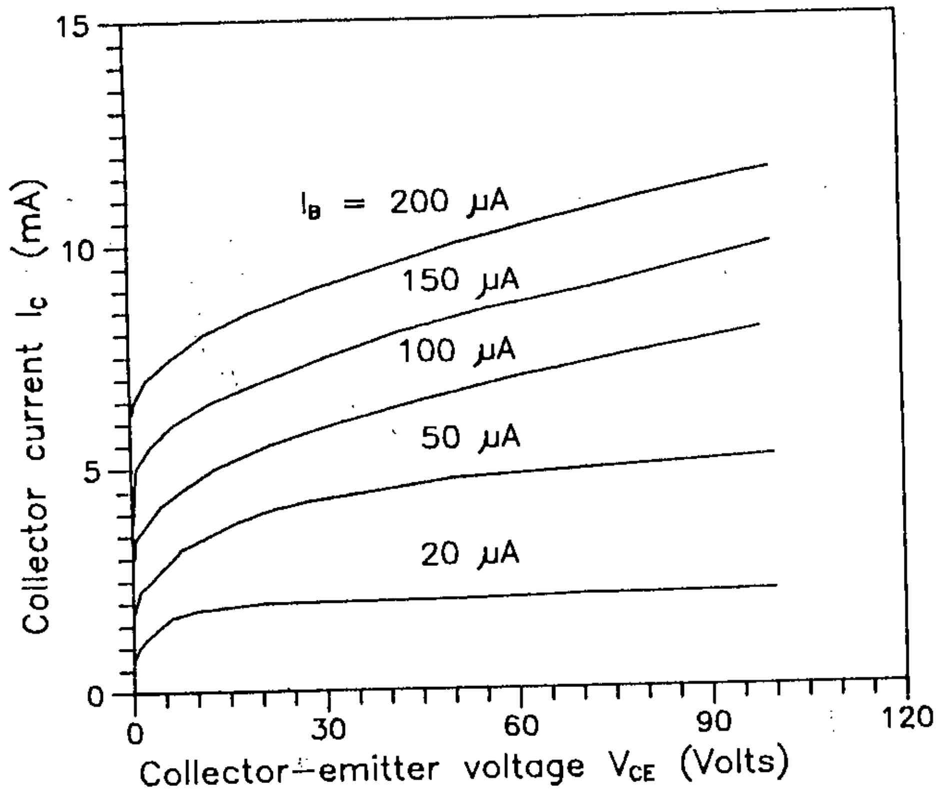

Fig. 3.2. Current–voltage characteristics for different base currents of a bipolar transistor.

and

$$V_{B'E} = V_T ln \frac{n_E N_B}{n_i^2} \tag{3.12}$$

We can see from equations (3.9)-(3.12) that for higher base currents $V_{B'E}$ increases which increases n_E. To keep V_{CE} constant, $V_{CB'}$ is decreased. Therefore, n_p also decreases which increases collector current. So, with constant V_{CE}, collector current with base currents. These plots also show that quasi-saturation occurs in a wider bias range if the base current is increased. This is because a larger base current results in a larger collector current in the collector and thus a larger voltage drop in the quasi-neutral collector, keeping the internal base-collector junction forward biased long after the external base-collector terminal is reverse biased.

Fig. 3.3 shows the collector current versus collector-emitter terminal voltage for different values of base-emitter terminal voltage $V_{B'E}$. From the characteristics we can see for same collector emitter voltage V_{CE}, collector current increases with $V_{B'E}$. This can be explain with the same equations above. For higher $V_{B'E}$, n_E increases and to keep V_{CE} constant, $V_{CB'}$ decreases with increase of $V_{B'E}$. So, n_p decreases and therefore, I_C increases.

Fig. 3.4. gives collector width as a function of collector-emitter voltage for given base current I_B at 50 μA and collector current I_C at 3.5 mA. It is found that with increasing collector width the collector-emitter voltage increases. A particular value of I_B fixes $V_{B'E}$ as clear from equation (3.11) and $V_{B'C}$ can be obtained from the collector current [19]. Now, the voltage drop accross epi-collector increases with W_C.

Fig. 3.5.. shows basewidth as a function of collector-emitter voltage for given values of collector and base currents. If base width increases then collector-emitter voltage also increases. For given I_B, the collector current will decrease with base width as I_C varies inversely with W_B. To keep I_C constant, the collector junction $V_{CB'}$ ($V_{CB'} > 0$) must be decreased with W_B, thereby decreases the injection region. The consequence of the decrease of width of the injection region is to increase V_{CE}.

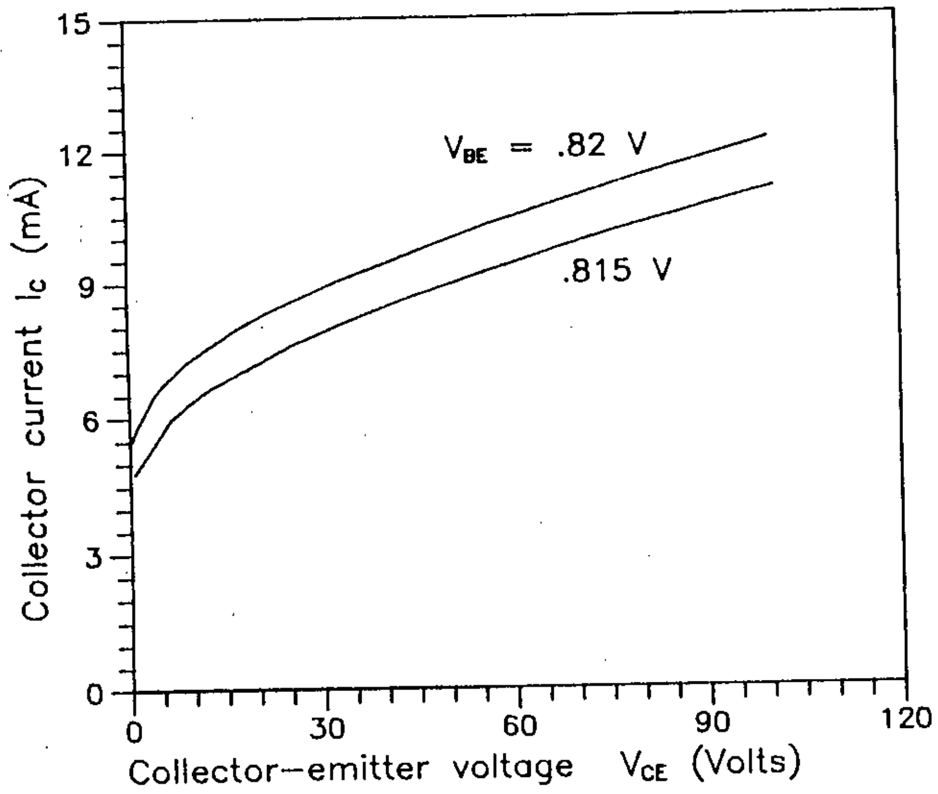

Fig. 3.3. Current-voltage characteristics of a bipolar transistor for different values of V_{BE}.

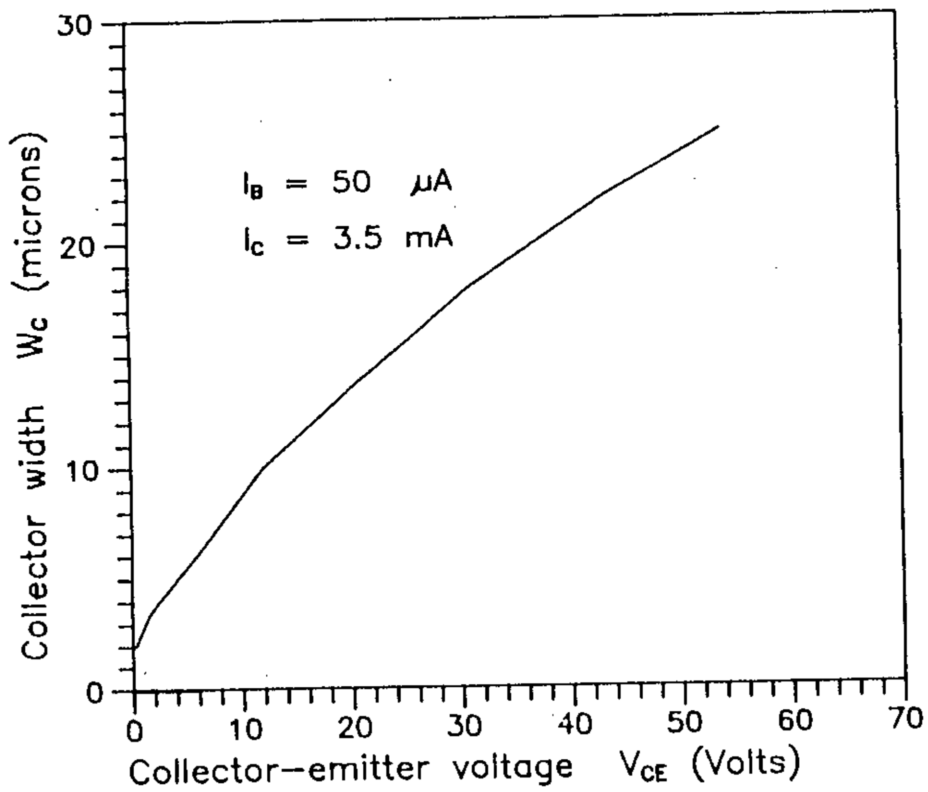

Fig. 3.4. Collector width as a function of collector−emitter voltage for given values of collector and base current of a bipolar transistor.

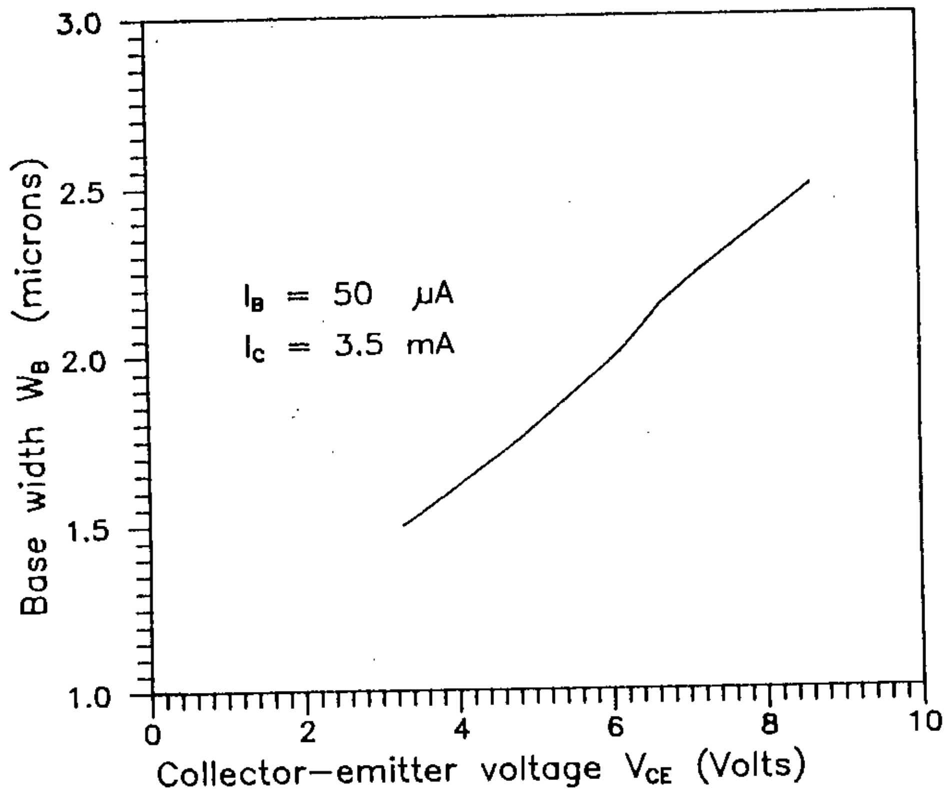

Fig. 3.5. Base width as a function of collector–emitter voltage for given values of collector and base current of a bipolar transistor.

Fig. 3.6. shows variation of collector-emiter voltage as a function of emiter width for given values of base and collector currents. The base current I_B decreases with W_E which is evident from equation (3.11). The $V_{EB'}$ need to be increased in order to obtain constant I_B against increase of W_E. The constant collector current decrease thereby increase of $V_{CB'}$ and consequently increases the injection region. This increase in injection regions results in decrease of V_{CE}.

Fig. 3.7 is the characteristics of emitter area as a function of collector-emitter voltage for given value of base and collector currents. Fig. 3.8 shows I_C-V_{CE} characteristics as a function of base current I_B calculated from the present model and obtained from measurements reported in Kull et.all [9]. The device make-up is given in table 1 and device parameters used in calculations are given in table 2. The results are agreed well with the measured value.

3.4 Conclusion

The different characteristics of an epitaxial $n^+pn^-n^+$ bipolar transistor are studied by using the present model. The model meets the requirements of minimum complexity for representation of the physical effects considered and has demonstrated its ability to simulate device behavior under dc operating condition. A computer program is developed based on algorithm illustrated in this chapter.

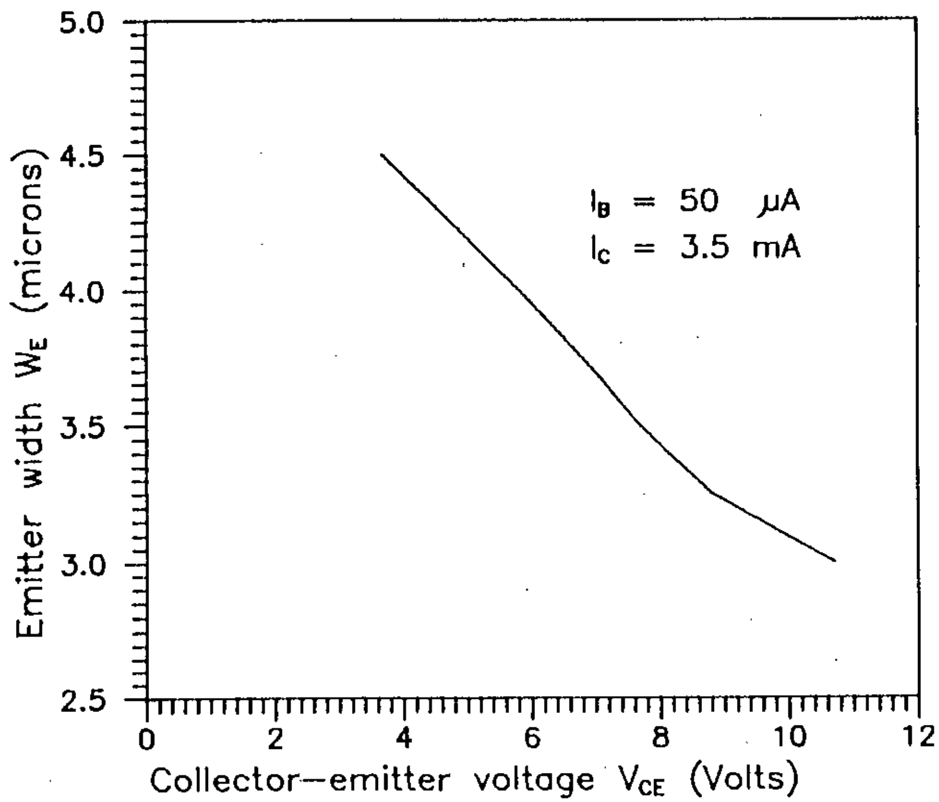

Fig.3.6. Emitter width as a function of collector–emitter voltage for given values of collector and base current of a bipolar transistor.

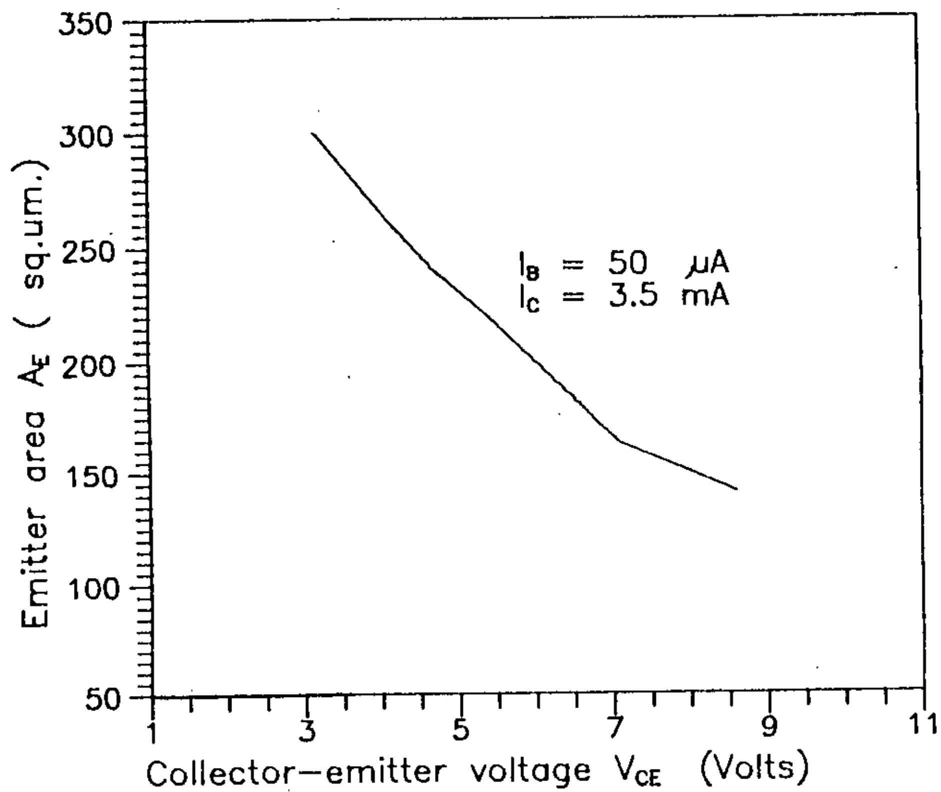

Fig. 3.7. Emitter area as a function of collector–emitter voltage for given values of collector and base currents of a bipolar transistor.

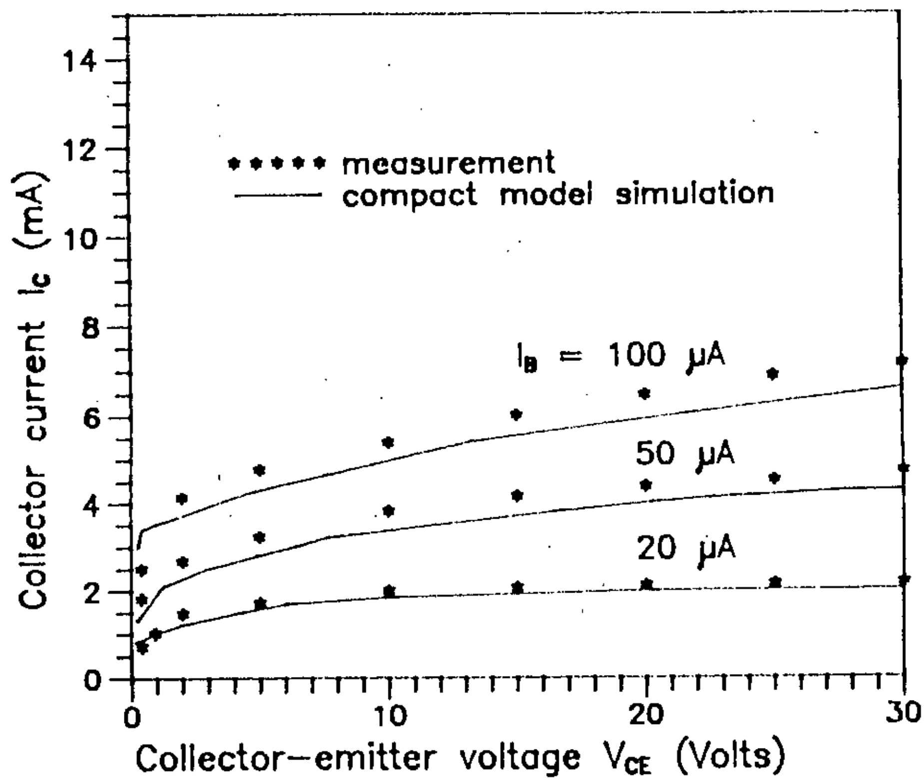

Fig. 3.8. Output characteristics comparing compact model simulation and measurements of an npn transistor [9].

For Collector Region		For Base Region	
D_n (cm^2/s)	μ_n ($cm^2/V.s$)	D_p (cm^2/s)	D_n (cm^2/s)
27	1075	10	20

Table 3.1 Device make-up

N_E (cm^{-3})	N_B (cm^{-3})	N_C (cm^{-3})	W_E (um)	A_e (um^2)	W_b (um)
10^{19}	4.5^{16}	10^{15}	3.7	180	2.15

Table 3.2 Device parameters

CHAPTER 4

Conclusions and Suggestions

4.1 Conclusions

Epitaxial $n^+pn^-n^+$ bipolar transistors are extensively used as power transistors, specially in high speed switch. Modelling of this type of transistor is important with its increased use. Device modelling aims at relating physical device parameters to device terminal characteristics. Simple and accurate device models are needed to predict the performances of the device. Models representing accurate transistors are complex and difficult to study. Therefore, there is a trade-off between accuracy and complexity. Different models have been analyzed till-date considering low and high level injection. But these models are not generally applicable specially at current densities exceeding space-charge limited current density. Therefore, an improved model based on physical principles is now essential for accurate simulation of this high current effects.

The collector of epitaxial bipolar transistor is more lightly doped than its base. As a result, high current effects occur predominantly in the lightly doped epitaxial collector region. At low voltages, the transistor operates in saturation and when the current is high, a space-charge region is formed in the lightly doped collector to support the current. In this research work, the dc current-voltage characteristics of a bipolar transistor have been modified based on the relevant device physics regarding the free carrier transport within the collector layer. The proposed model covers the saturation , quasi-saturation and active mode operations. The model is simple in representing the physical effects and has demonstrated its ability to

simulate device behaviour under dc operating conditions. The present model does not require parameters extracted from measurements. The results obtained by the model simulation are in good agreement with the measurements reported in the literature.

4.2 Suggestions

In the proposed model, minority carrier current in the epitaxial collector has been neglected. Hence, the model can be improved by taking into consideration the minority carrier current in the epitaxial collector region. Another limitation of this model is that, the flow of current through the transistor has been considered to be one-dimensional. Further modification of the model can be done considering two dimensional case.

REFERENCES

[1] Ph. Leturcq, "Power bipolar devices," Microelectronics and Reliability, Vol. 24, No. 2, 1984, pp. 313-337.

[2] J. J. Ebers and J. L. Moll, "Large-signal behavior of junction transistors," Proc. IRE, Vol.42, No. 12, 1954, pp. 1761-1772.

[3] R. Beaufoy and J. J. Sparkes, "The junction transistor as a charge-controlled device," ATE J. (London), 13, No. 4, 1957, pp. 310-324.

[4] J. M. Early, "Effects of space charge layer widening in junction transistors," Proc. IRE, 40, No. 11, 1952, pp. 1401-1406.

[5] C. T. Sah, R. N. Noyce and W. Shockly, "Carrier generation and recombination in p-n junctions and p-n junctions characteristics," Proc. IRE 45, No. 9, 1957, pp. 1228-1243.

[6] W. M. Webster, "On the variation of junction transistor current gain amplification factor with emitter current," Proc. IRE, 42, No. 6, 1954, pp. 914-920.

[7] Jr. C. T. kirk, "A theory of transistor cutoff frequency (f_T) falloff at high current densities," IRE Trans. on Electron Devices, ED-9, No. 2, 1962, pp. 164-174.

[8] H.K. Gummel and H. C. Poon, "An integral charge control model of bipolar transistors," The Bell System Technical Journal, Vol. 49, 1970, pp. 827-852.

[9] G. M. Kull, L. W. Nagel, S. W. Lee, P. Lloyd, J. Prendergast and H. Dirks, "Unified circuit model for bipolar transistors including quasi-saturation effects," IEEE Trans. on Electron Devices, Vol. ED-32, No. 6, 1985, pp. 1103-1113.

[10] L. E. Clark, "Characteristics of two-region saturation phenomena," IEEE Trans. on Electron Devices, Vol. ED-16, 1969, pp.113-116.

[11] R. J. Whitter and D. A. Tremere, "Current gain and cut-off frequency fall off at high currents," IEEE Trans. on Electron Devices, Vol. ED-16, 1969, pp. 39-59.

[12] W. J. Chudobiak, "The saturation characteristics of n-p-ν-n power transistors," IEEE Trans. on Electron Devices, Vol. ED-17, 1970, pp. 843-852.

[13] P. L. Hower, "Application of a charge-control model to high voltage power transistors," IEEE Trans. on Electron Devices, Vol. ED-23, 1965, pp. 863-870.

[14] R. Kumar and L. P. Hunter, "Collector capacitance and high-level injection effects in bipolar transistors," IEEE Trans. on Electron Devices, Vol. ED-22, 1975, pp. 51-60.

[15] J. Hanggeun and J. G. Fossum, "Physical modeling of high-current transients for bipolar transistor circuit simulation," IEEE Trans. on Electron Devices, Vol. ED-34, No.4, 1987, pp. 898-905.

[16] V. Gianfranco, "The effects of carrier accumulation at the cathode on the negative resistance induced by avalanche injection in silicon bulk devices," Solid-state Electronics, 18, 1975, pp. 1123-1130.

[17] H. C. Graaff, W. J. Kloosterman and Schmitz, "The emitter efficiency of bipolar transistors," Solid-State Electronics, 22, 1977, pp. 515-521.

[18] G. E. Possin, M. S. Alder and B. J. Baliga, "Measurements of the pn product in heavily doping epitaxial emitters," IEEE Trans. on Electron Devices, ED-31, 1984, pp.3-7.

[19] G. A. M. Hurkx, "An improved analytical description of the effect of velocity saturation on the collector current of a bipolar transistor," Solid-State Electronics, 35, 1992, pp. 1397-99.

[20] J. W. Slotboom and H. C. Graaff, "Measurements of bandgap narrowing in Si bipolar transistors," Solid-State Electronics, 19, 1976, pp. 857-862.

[21] H. C. Graaff and W. J. Kloosterman, "New formulation of the current and charge relations in bipolar transistor for modeling for CACD purposses," IEEE Trans. on Electron Devices, ED-32, 1985, pp. 1415-1419.

APPENDIX

Mathematical Expressions for Minority Carriers at Junction Edges

The law of junctions can be written in the generalized forms as,

$$\frac{n_p(0)}{n_n(0)} = \frac{n_{po}}{n_{no}} e^{V_j/V_T}$$

and

$$\frac{p_n(0)}{p_p(0)} = \frac{p_{no}}{p_{po}} e^{V_j/V_T}$$

where, V_j is the voltage across the junction.

The minority carrier at the base side edge of the collector-base junction can be derived using the above equations and can be written as,

$$n_p = \left(\frac{n_i^2}{N_B}\right)\left(\frac{n_n}{N_C}\right) e^{-V_{CB'}/V_T} \tag{A1}$$

and also from law of mass action,

$$n_p p_p = n_n p_n \tag{A2}$$

Considering the charge-neutrality condition in base and collector,

it can be shown from eqns.(A1) and (A2),

$$p_n = A^2 n_n e^{-2V_{CB'}/V_T} + A e^{-V_{CB'}/V_T} N_B \tag{A3}$$

where, $A = \left(\frac{n_i^2}{N_B}\right)\frac{1}{N_C}$.

The solution of the equation (A3) in p_n is,

$$p_n = \frac{AN_B\left[1 + A\frac{N_C}{N_B}e^{-V_{CB'}/V_T}\right]\exp(-V_{CB'}/V_T)}{1 - A^2 e^{-2V_{CB'}/V_T}} \tag{A4}$$